

511-32

185871

TDA Progress Report 42-114

August 15, 1993

P-10

N94-14380

Enhanced Decoding for the Galileo S-Band Mission

S. Dolinar and M. Belongie
Communications Systems Research Section

A coding system under consideration for the Galileo S-band low-gain antenna mission is a concatenated system using a variable redundancy Reed-Solomon outer code and a (14,1/4) convolutional inner code. The 8-bit Reed-Solomon symbols are interleaved to depth 8, and the eight 255-symbol codewords in each interleaved block have redundancies 64, 20, 20, 20, 64, 20, 20, and 20, respectively (or equivalently, the codewords have 191, 235, 235, 235, 191, 235, 235, and 235 8-bit information symbols, respectively). This concatenated code is to be decoded by an enhanced decoder that utilizes (1) a maximum likelihood (Viterbi) convolutional decoder; (2) a Reed-Solomon decoder capable of processing erasures; (3) an algorithm for declaring erasures in undecoded codewords based on known erroneous symbols in neighboring decodable words; (4) a second Viterbi decoding operation (redecoding) constrained to follow only paths consistent with the known symbols from previously decodable Reed-Solomon codewords; and (5) a second Reed-Solomon decoding operation using the output from the Viterbi redecoder and additional erasure declarations to the extent possible.

It is estimated that this code and decoder can achieve a decoded bit error rate of 1×10^{-7} at a concatenated code signal-to-noise ratio of 0.76 dB. By comparison, a threshold of 1.17 dB is required for a baseline coding system consisting of the same (14,1/4) convolutional code, a (255,223) Reed-Solomon code with constant redundancy 32 also interleaved to depth 8, a one-pass Viterbi decoder, and a Reed-Solomon decoder incapable of declaring or utilizing erasures. The relative gain of the enhanced system is thus 0.41 dB.

It is predicted from analysis based on an assumption of infinite interleaving that the coding gain could be further improved by approximately 0.2 dB if four stages of Viterbi decoding and four levels of Reed-Solomon redundancy are permitted. Confirmation of this effect and specification of the optimum four-level redundancy profile for depth-8 interleaving is currently being done.

I. Introduction

This article looks at the performance of a Reed-Solomon plus convolutional concatenated coding system with enhanced decoding as planned for the Galileo S-band low-gain antenna (LGA) mission. The baseline system without enhanced decoding uses a (255,223) Reed-Solomon outer code concatenated with a (14,1/4) convolutional inner code, and interleaves the Reed-Solomon symbols to depth 8. The convolutionally encoded symbols are decoded by maximum likelihood (Viterbi) decoding, and each Reed-Solomon codeword is decoded algebraically to correct a maximum of sixteen 8-bit symbols per 255-symbol word. There are two types of decoding enhancements planned for the Galileo LGA mission: *Reed-Solomon redecoding* using erasure declarations and *Viterbi redecoding* using Reed-Solomon corrected symbols.

Reed-Solomon redecoding is possible when at least one but fewer than eight of the codewords within a block of eight interleaved words is decodable (correctable). The Reed-Solomon decoder can then extrapolate the locations of corrected errors in the decodable word(s) to neighboring locations in adjacent undecodable word(s) and declare the corresponding symbols to be erased. The basis for this error extrapolation or *error forecasting* is that errors from the Viterbi decoder tend to occur in bursts that are often longer than the 8-bit Reed-Solomon symbols. If the erased symbols are highly likely to be erroneous, then the undecoded words might be decoded by a second try at Reed-Solomon decoding that utilizes the erasure information.

Viterbi redecoding consists of an extra pass through a maximum likelihood decoder that is now constrained to follow only paths consistent with the known symbols from previously decodable Reed-Solomon codewords. The Viterbi redecoder is much less likely to choose a long erroneous path because any path under consideration is pinned to coincide with the correct path at the location(s) of the known symbols.

Both redecoding processes may be repeated an arbitrary number of times (with diminishing returns). Repetitions of Reed-Solomon redecoding allow the testing of several different combinations of reasonable error extrapolations from the known error locations, and can be accomplished relatively cheaply, as Reed-Solomon decoding is much faster than Viterbi decoding. Each repetition of Viterbi redecoding requires a whole new *decoding stage*: it must begin with the output from the previous Reed-Solomon decoding stage and must feed its output to another following Reed-Solomon stage.

With both types of redecoding, it usually pays to put different amounts of redundancy in neighboring Reed-Solomon codewords. Words with high redundancy can be counted on to decode during an initial decoding try, and the information from these decoded words can be used to assist the decoding of codewords with lower redundancy later.

In this article, the stages of the enhanced decoding process are denoted as follows:

- VIT-1 the first pass of the raw data through the Viterbi decoder.
- RS-1 the first pass of the Viterbi decoded bits through the Reed-Solomon decoder, including the possibility of several trials per codeword using erasure declarations forecast from previously decoded codewords.
- VIT-2 the second pass of the raw data through the Viterbi decoder, aided this time by known bits from codewords successfully decoded in RS-1.
- RS-2 the pass of the Viterbi redecoded bits from VIT-2 through the Reed-Solomon decoder, again using erasure declarations to assist in decoding previously undecodable codewords.
- ⋮
- VIT- n the n th pass of the raw data through the Viterbi decoder, aided this time by known bits from codewords successfully decoded in RS- $(n - 1)$.
- RS- n the pass of the Viterbi redecoded bits from VIT- n through the Reed-Solomon decoder, again using erasure declarations to assist in decoding previously undecodable codewords.

II. Three Analysis Approaches

The analysis in this article is first performed using an assumption of infinite interleaving and no Reed-Solomon erasure declarations. This is done for one, two, and four Viterbi decoding stages. A calculation is made of the maximum coding gain obtainable by adding the extra stages. With the infinite interleaving assumption, concatenated system performance can be accurately obtained to error rates of 1×10^{-7} or lower, based on megabits of simulated Viterbi decoder data.

The analysis then continues for the actual Galileo conditions with depth-8 interleaving but still no Reed-Solomon erasure declarations. This analysis cannot directly verify 1×10^{-7} error rates even with gigabits of Viterbi decoded data, but extrapolated performance curves for depth-8 interleaving can be relied on with high confidence because of their similarity to certain corresponding curves derived under the infinite interleaving assumption.

Finally, the depth-8 interleaving analysis is extended to allow Reed-Solomon erasure declarations using a simple error forecasting strategy.

The analysis in this article characterizes the concatenated decoding system based on the usual assumption that the received symbols are corrupted by stationary additive white Gaussian noise. No attempt has been made to refine the decoder models to account for effects due to such factors as imperfect arraying, phase drifts, or time-varying signal-to-noise ratio.

III. Analysis Based on Infinite Interleaving and No Erasure Declarations

This section analyzes the gains possible from Viterbi redecoding alone, without Reed-Solomon erasure declarations, but using an assumption of infinite interleaving. It begins with a baseline analysis of one-stage decoding (no redecoding) and proceeds to evaluate the gains possible from using two stages and four stages.

A. One-Stage Decoding

One-stage decoding for this case consists of one pass through the Viterbi decoder followed by one pass without erasure declarations through the Reed-Solomon decoder. The performance of the Viterbi decoder is evaluated by simulation, and that of the Reed-Solomon decoder is calculated from a formula.

1. Stage VIT-1. The Viterbi decoder for the Galileo (14,1/4) convolutional code is characterized by the performance curves given in Fig. 1. The curves show Viterbi decoder bit error rate BER and 8-bit Reed-Solomon symbol error rate SER as functions of the signal-to-noise ratio E_b/N_o of the convolutional code. The points on these curves are based on about 2 Gbits of data each in the range from 0.0 to 0.5 dB, and on more than 400 Mbits each in the range from 0.6 dB to 1.0 dB (but 2 Gbits at 0.7 dB). All of the data were decoded by the Big Viterbi Decoder (BVD).

Figure 1 shows that the (14,1/4) Galileo LGA code achieves a BER of 5×10^{-3} at an E_b/N_o of 0.65 dB. By comparison, Tables 1 and 2 of [1] show that the (15,1/4) Galileo high-gain antenna (HGA) code achieves a BER of 5×10^{-3} at an E_b/N_o of 0.52 dB. The (14,1/4) LGA code is 0.13 dB inferior to the (15,1/4) HGA code at this error rate.

2. Stage RS-1. Figure 2 shows the performance of the Reed-Solomon decoder under an assumption of infinite interleaving and no erasure declarations, but with varying amounts of error correction E (or codeword redundancy $2E$). The E values for the various curves are labeled along the right and bottom edges of the graph. These curves are based on the same BVD simulation runs described for Stage VIT-1. On this figure, and on all succeeding figures, the signal-to-noise ratio E_b/N_o on the x-axis is the same as that in Fig. 1, i.e., the signal-to-noise ratio for the inner convolutional code alone. Thus, these curves cannot be used for a direct reading of the optimum value of E for single-stage Reed-Solomon decoding because they do not reflect the increasing dilution of signal energy due to increasing redundancy of the Reed-Solomon code. However, this latter adjustment is a simple numerical computation, and presenting a parametric family of performance curves as those in Fig. 2 leads to effective trial-and-error optimization methods for the multistage decoding processes analyzed below.

The curves in Fig. 2, and in all succeeding figures, show the Reed-Solomon decoded 8-bit SER rather than the decoded BER . This is a convenience because the analysis of future decoding stages depends primarily on SER rather than BER . The BER is slightly less than half the corresponding SER , as can be seen by comparison of the BER and SER curves in Fig. 1.

3. Performance of One-Stage Decoding. For the baseline coding system using the (255,223) Reed-Solomon code, E is 16 and a one-stage decoding system with infinite interleaving can achieve an SER of 2×10^{-7} (i.e., a BER of $\sim 1 \times 10^{-7}$) at convolutional code $E_b/N_o = 0.52$ dB. The corresponding concatenated code signal-to-noise ratio is $E_b/N_o = 1.10$ dB, accounting for the 0.58 dB redundancy of the (255,223) Reed-Solomon code.

Alternatively, if a (255,231) Reed-Solomon code with $E = 12$ had been used, the required convolutional code operating point would move to $E_b/N_o = 0.67$ dB, but the corresponding concatenated code signal-to-noise ratio would stay at $E_b/N_o = 1.10$ dB, because the redundancy of the (255,231) Reed-Solomon code is only 0.43 dB. In fact, the lowest required concatenated code signal-to-noise

ratio of approximately 1.10 dB is achieved over a range of values of E from 12 to 16, or equivalently over a range of convolutional code operating points E_b/N_o from 0.52 dB to 0.67 dB.

B. Two-Stage Decoding

Two-stage decoding consists of two passes each through the Viterbi decoder and the Reed-Solomon decoder. The only difference in the decoding algorithms is that the Viterbi decoder on the second pass is constrained to follow only paths consistent with known symbols from Reed-Solomon codewords that were decoded on the first pass. The Reed-Solomon decoding algorithm is unchanged for both passes.

1. Stage VIT-1. The output of Stage VIT-1 is characterized by the same performance curves given in Fig. 1.

2. Stage RS-1. The output of Stage RS-1 is characterized by the same performance curves given in Fig. 2. However, now it is important to utilize the full set of information contained in all the curves in Fig. 2 rather than just to focus on the values of E from 12 to 16 that give optimum one-stage performance.

3. Stage VIT-2. The performance of Stage VIT-2 is dependent on how often known 8-bit symbols from the previous Reed-Solomon decoding are inserted into the Viterbi decoder data stream. If the Reed-Solomon code has constant redundancy, the known symbols will occur with a certain average frequency (determined by the corresponding SE R curve in Fig. 2), but not according to any repeating pattern. If the Viterbi redecoder had to contend with only randomly occurring unknown symbols interspersed with probability SE R $< 10^{-1}$ into a stream of mostly known symbols, Stage VIT-2 would produce an almost perfect output at any E_b/N_o shown in Fig. 2. However, even with infinite interleaving, Stage RS-1 decoding failures will be correlated from one codeword to the next due to the burstiness of the errors from Stage VIT-1. Therefore, the Viterbi redecoder is likely to encounter strings of unknown symbols of unpredictable length. Long strings of unknown symbols will locally negate the value of the otherwise highly likely known symbols and cause correspondingly long strings of redecoded errors. No effective analytical techniques have been developed to quantitatively assess the performance of Stage VIT-2 after decoding a constant redundancy code in Stage RS-1.

If the Reed-Solomon codewords have variable redundancy and there is an appreciable difference in redundancy values, then it is possible (and reasonable) to set

the E_b/N_o operating point so that the most highly redundant codewords are almost certain to decode, while the less redundant codewords are undecodable with probability much higher than the target error probability for the multistage decoding process. Then, to a good conservative approximation, it can be assumed that the known symbols from Stage RS-1 will occur in at least the same repeating pattern as the pattern of the most highly redundant codewords. Under these conditions, the performance of Stage VIT-2 can be effectively parameterized by feeding the Viterbi redecoder various repeating patterns of known symbols.

Viterbi redecoded BER and SE R tables were presented in [2] for three different known symbol patterns (one in two, one in four, and one in eight) and three different convolutional codes (the (7,1/2) NASA standard code, an (11,1/4) code, and the (15,1/4) Galileo HGA code). A similar analysis for the (14,1/4) Galileo LGA code was performed for this article, and the SE R results are shown in Fig. 3. These curves are based on slow-running software simulations of only about 1 Mbit each, because the high-rate BVD used to generate the 2-Gbit samples for Stage VIT-1 could not without modification incorporate the known symbol information into its decoding process.

Figure 3 shows multiple curves for the one-in-four and one-in-eight known symbol cases, because, as noted in [2], the redecoded SE R depends on the symbol's phase relative to the position of the nearest known symbol in the pattern. It can be argued theoretically and has been confirmed by simulation that phases $\pm n$ have approximately the same SE R, so the curves in Fig. 3 represent averages of the simulated SE R values for $\pm n$ ($n = 1, 2$ for the one-in-four case and $n = 1, 2, 3, 4$ for the one-in-eight case).

Figure 3 has two different labels for its y-axis. The label on the left is the actual SE R observed from the simulation runs. The label on the right is the equivalent convolutional code E_b/N_o that produces the same SE R values without any known symbols, i.e., the convolutional code signal-to-noise ratio that would have been required to produce the same SE R with one-stage Viterbi decoding.

4. Stage RS-2. The output of Stage RS-2 is characterized by the same family of performance curves given in Fig. 2. Under the infinite interleaving assumption, all symbols in a given codeword are independent, so the decoding error rate depends only on the SE R from Viterbi decoding during Stage VIT-2. Thus, the curves in Fig. 2 are directly applicable to the determination of the performance of Stage RS-2 if the equivalent one-stage E_b/N_o values are used to characterize the output of Stage VIT-2.

For example, suppose that every fourth codeword is *strong* (i.e., highly redundant) and can be presumed to decode with high probability during Stage RS-1. Then for Stage VIT-2, there are known symbols spaced four symbols apart, and the curves labeled 1/4 and 2/4 in Fig. 3 are applicable. If the convolutional code operating point is $E_b/N_o = 0.20$ dB, then the equivalent Stage VIT-1 operating point is 0.85 dB for symbols at phases ± 1 and 0.77 dB for symbols at phase ± 2 . If a Reed-Solomon code with $E = 9$ is used for the remaining weak (i.e., less redundant) codewords, Fig. 2 shows that the SE_R for the weak codewords is approximately 1×10^{-7} for codewords at phases ± 1 and 1×10^{-6} for codewords at phase ± 2 .

5. Performance of Two-Stage Decoding. The overall performance of two-stage decoding depends on the likelihood of decoding both the strong codewords during Stage RS-1 and the weak codewords during Stage RS-2. The SE_R of the strong codewords can be conservatively presumed to equal the SE_R from Stage RS-1 for a code with the redundancy of the strong codewords. There are two contributions to the SE_R of the weak codewords. Weak codewords will fail to decode when the number of symbol errors from the redecoding stage exceeds the weak codewords' correction capability. Furthermore, weak codewords may not successfully decode whenever neighboring strong codewords do not decode during Stage RS-1. In this article, it is assumed that this second contribution to the SE_R of weak codewords equals the SE_R of the strong codewords. This leads to an approximate formula for the overall SE_R of the form $SE_R = SE_{R_s}(1) + f_w SE_{R_w}(2)$, where $SE_{R_s}(1)$ is the strong codewords' symbol error rate after Stage RS-1; $SE_{R_w}(2)$ is the weak codewords' symbol error rate after Stage RS-2, assuming known symbols during Stage VIT-2 from neighboring decodable strong codewords; and f_w is the fraction of weak codewords. If the weak codewords do not all have equivalent performance, the second term of this formula can be generalized to include a sum of contributions from each individual type of weak codeword, weighted by the fraction of each type.

If the target SE_R is 2×10^{-7} , then both $SE_{R_s}(1)$ and $SE_{R_w}(2)$ should be reduced to roughly 1×10^{-7} . Building upon the example introduced in the previous section with one strong codeword every four, Fig. 2 shows that a Stage RS-1 correction capability of $E = 30$ is required to bring $SE_{R_s}(1)$ to 1×10^{-7} at a convolutional code operating point of $E_b/N_o = 0.20$ dB. Similarly, the discussion of the previous example noted that $SE_{R_w}(2)$ could be brought to 1×10^{-7} for the weak codewords at phases ± 1 by using a Reed-Solomon code with a correction capability of $E = 9$. For the weak codewords at phase ± 2 , $E = 9$ is insufficient because the resulting $SE_{R_w}(2)$ of

1×10^{-6} would raise the overall SE_R above 2×10^{-7} all by itself. However, $E = 10$ yields $SE_{R_w}(2) = 2 \times 10^{-7}$ for the weak codewords at phase ± 2 , resulting in an overall $SE_R = 1 \times 10^{-7} + (1/2)1 \times 10^{-7} + (1/4)2 \times 10^{-7} = 2 \times 10^{-7}$. The *redundancy profile* for this codeword set is $2E = (60, 18, 20, 18)$, which corresponds to an average code rate of 229/255, or 0.52 dB of overhead for the Reed-Solomon code. The corresponding concatenated code operating point is $E_b/N_o = 0.20$ dB + 0.52 dB = 0.72 dB. This represents an improvement of 0.38 dB relative to the required operating point for the one-stage decoder.

If the target SE_R is still 2×10^{-7} but the convolutional code operating point is moved to 0.10 dB, the required strong codeword correction capability to achieve $SE_R = 1 \times 10^{-7}$ in Stage RS-1 is now $E = 36$. After Viterbi redecoding with one in four symbols known, the SE_R -equivalent Stage VIT-1 operating points from Fig. 2 are 0.79 dB for phases ± 1 and 0.72 dB for phase ± 2 . Weak-codeword correction capabilities of $E = 10$ and $E = 11$ are sufficient to bring the corresponding $SE_{R_w}(2)$ values to 1×10^{-7} and 2×10^{-7} , respectively. The overall $SE_R = 1 \times 10^{-7} + (1/2)1 \times 10^{-7} + (1/4)2 \times 10^{-7} = 2 \times 10^{-7}$, as before. The redundancy profile of this codeword set is $2E = (72, 20, 22, 20)$, which corresponds to an average code rate of 443/510, or 0.61 dB of overhead for the Reed-Solomon code. The corresponding concatenated code operating point is $E_b/N_o = 0.10$ dB + 0.61 dB = 0.71 dB, which is almost exactly the same as before. As for the case of one-stage decoding, there is a range of convolutional code operating points over which the same near-optimal concatenated code performance can be achieved by appropriately adjusting the Reed-Solomon redundancies.

The case of one strong codeword every two is not directly analyzable from Fig. 2 because the equivalent convolutional code E_b/N_o is outside the range of values measured for Fig. 2. However, calculations show that for SE_R in the range of 0.0006 to 0.0009, a Reed-Solomon code with $E = 4$ will bring the SE_R for Stage RS-2 under 1×10^{-7} , but with $E = 3$ it is above 3×10^{-7} . Referring to Fig. 3 for the Stage VIT-2 SE_R values after redecoding with one in two symbols known, $E = 4$ will be required for the weak codewords if the convolutional code operating point is beyond about 0.1 dB. Because of the large spacing between the $E = 4$ and the $E = 3$ curves, it can be argued that $E = 3$ remains inadequate for a few tenths of a dB beyond 0.1 dB (and beyond the region in Fig. 3 for which simulation results have been obtained thus far). The choice of E for the strong codewords depends on the convolutional code operating point. For example, $E = 30$ is required at 0.20 dB, while $E = 25$ is sufficient at 0.30 dB. The corresponding redundancy profiles (60,8) and (50,8) con-

tribute Reed-Solomon coding overheads of 0.62 dB and 0.52 dB, respectively, and both of the resulting concatenated code operating points are $E_b/N_o = 0.82$ dB. This is about 0.1 dB worse than the best operating point obtainable with the scheme that uses only one strong codeword every four. It reflects the inefficiency of investing high amounts of Reed-Solomon redundancy in codewords spaced so closely together that the Stage VIT-2 SE_R in Fig. 3 is driven lower than necessary.

The case of one strong codeword every eight blurs the distinction between strong and weak codewords because of the relatively wide variation in Stage VIT-2 SE_R among the various possible symbol phases. For example, at 0.20 dB a code with $E = 30$ will bring the strong codeword SE_R to 1×10^{-7} . From Fig. 3, the SE_R -equivalent operating points for the weak codewords after Viterbi decoding are 0.67 dB, 0.51 dB, 0.43 dB, and 0.41 dB for phases $\pm 1, \pm 2, \pm 3$, and ± 4 , respectively, requiring $E = 12, 17, 19$, and 20, respectively, to bring the individual $SE_{R_w}(2)$ values to the range of 1×10^{-7} to 2×10^{-7} , and the resulting overall SE_R to approximately 2×10^{-7} . The corresponding redundancy profile (60, 24, 34, 38, 40, 38, 34, 24) costs 0.67 dB, which moves the concatenated code operating point to 0.87 dB. This is inferior to both the cases of one-in-four and the one-in-two strong codewords.

All of the performance results discussed in this section for two-stage decoding have been obtained by trial-and-error optimization using Figs. 2 and 3, and they may not always reflect the exact optimum performance. However, because the concatenated code operating point stays relatively constant (within a couple hundredths of a dB) over a relatively large range of convolutional code operating points (at least a tenth of a dB), the trial-and-error method gives results accurate to a few hundredths of a dB wherever data are available.

C. Four-Stage Decoding

Four-stage decoding consists of four passes each through the Viterbi decoder and the Reed-Solomon decoder. The main difference relative to two-stage decoding is that now it is profitable to design four separate levels of Reed-Solomon codeword redundancies rather than two. The analysis proceeds as in the two-stage case.

1. **Stage VIT-1.** The output of Stage VIT-1 is characterized by the performance curves given in Fig. 1.

2. **Stages RS-1, RS-2, RS-3, and RS-4.** The outputs of Stages RS-1, RS-2, RS-3, and RS-4 are characterized by the performance curves given in Fig. 2.

3. **Stages VIT-2, VIT-3, and VIT-4.** The outputs of Stages VIT-2, VIT-3, and VIT-4 are characterized by the performance curves given in Fig. 3.

4. **Performance of Four-Stage Decoding.** With four-stage decoding, it pays to design four different categories of Reed-Solomon codewords, not just strong and weak. As an example, one codeword out of every eight could be assigned the highest redundancy, and these codewords could be expected to decode during Stage RS-1; one of eight could be assigned the next highest redundancy (spaced halfway between the highest redundancy words) and these could be expected to decode during Stage RS-2 after Stage VIT-2 Viterbi decoding, using a pattern of one known symbol every eight. Then the third highest redundancy words (one of every four spaced halfway between the two types of higher redundancy words) will be decoded in Stage RS-3 after Stage VIT-3 Viterbi decoding with the help of one known symbol every four; finally, the lowest redundancy words (one of every two) will be decoded in Stage RS-4 after Stage VIT-4 Viterbi decoding using one known symbol every two. A scheme of this sort was proposed in [2] for the Galileo HGA convolutional code and other codes.

The overall SE_R for this scheme can be calculated as in the two-stage case by assuming that the SE_R for the codewords that are supposed to decode during a particular stage also contributes to the SE_R for all weaker codewords. The resulting formula for the overall SE_R is of the form $SE_R = SE_{R_a}(1) + 7/8 SE_{R_b}(2) + 3/4 SE_{R_c}(3) + 1/2 SE_{R_d}(4)$, where the indices a, b, c, d , refer to the strongest, next strongest, third strongest, and weakest codewords and (n) refers to decoding during Stage RS- n , $n = 1, 2, 3, 4$.

To achieve an overall SE_R of 2×10^{-7} , it is necessary that all four terms in the expression for SE_R be driven to approximately 10^{-7} or lower. At a convolutional code operating point of 0.10 dB, the equivalent operating points for Stages VIT-2 and VIT-3 are 0.33 dB and 0.72 dB, respectively, from the curves for phase ± 4 of 8 and phase ± 2 of 4 in Fig. 3. An appropriate set of E values to drive $SE_{R_a}(1)$, $SE_{R_b}(2)$, and $SE_{R_c}(3)$ each below 1×10^{-7} is $E = 36, 24$, and 12. As in the earlier discussion, the SE_R -equivalent output of Stage VIT-4 is beyond the scale of Fig. 2, but separate calculations show that $E = 4$ is sufficient to bring $SE_{R_d}(4)$ under 1×10^{-7} and, together with the three aforementioned values, to achieve an overall SE_R of about 2×10^{-7} . The corresponding redundancy profile (72, 8, 24, 8, 48, 8, 24, 8) costs 0.45 dB, and so the concatenated code operating point is $E_b/N_o = 0.10$ dB + 0.45 dB = 0.55 dB.

If the convolutional code operating point is lowered to 0.00 dB, the *SER* for phase ± 1 of 2 is no longer small enough to permit $E = 4$ for the lowest redundancy code-words, but $E = 5$ is sufficient. From Fig. 3 the intermediate *SER*-equivalent convolutional code operating points are 0.27 dB and 0.66 dB. An appropriate set of E values to achieve an overall *SER* of about 2×10^{-7} is $E = 43, 27, 13,$ and 5 . The corresponding redundancy profile (86, 10, 26, 10, 54, 10, 26, 10) costs 0.52 dB, and the concatenated code operating point is $E_b/N_o = 0.00 \text{ dB} + 0.52 \text{ dB} = 0.52 \text{ dB}$. This represents a slight improvement over the 0.10 dB convolutional code operating point, and there may be a slightly better operating point in the unsimulated region below 0.00 dB.

IV. Analysis Based on Depth-8 Interleaving and No Erasure Declarations

The analysis now continues for the actual Galileo conditions with depth-8 interleaving. As with the infinite interleaving analysis presented earlier, this section begins with a baseline analysis of one-stage decoding (no Viterbi redecoding) and proceeds to evaluate the gains possible from using a second stage. Results are not presented for more than two decoding stages.

A. One-Stage Decoding

For one-stage decoding with depth-8 interleaving, the performance of the Viterbi decoder is the same as before. The performance of the Reed-Solomon decoder must be evaluated by directly measuring the probability of decoder failure on simulated interleaved output from the Viterbi decoder.

1. **Stage VIT-1.** The output of Stage VIT-1 is characterized by the performance curves given in Fig. 1.

2. **Stage RS-1.** Figure 4 shows the performance of the Reed-Solomon decoder under an assumption of depth-8 interleaving and no erasure declarations, with varying amounts of error correction $E = 4, 10, 16, 32,$ and 34 . The depth-8 interleaving curves are plotted against a backdrop "grid" of infinite interleaving curves from Fig. 2.

In Fig. 4, the performance curves for depth-8 interleaving are shifted slightly to the right with respect to the corresponding infinite interleaving curves, showing a slight degradation due to nonideal interleaving of less than 0.05 dB at *SER* values around 1×10^{-5} or so. Equivalently, this degradation may be characterized as an approximate reduction in the error correction capacity of the Reed-Solomon code. For example, the depth-8 curve for

$E = 16$ starts out coincident with the $E = 16$ infinite interleaving curve for high *SER*, but gradually drifts to cross the $E = 15$ infinite interleaving curve at an *SER* of $\sim 1 \times 10^{-3}$, and appears headed to cross the $E = 14$ infinite interleaving curve at an *SER* of $\sim 1 \times 10^{-7}$. Thus, depth-8 interleaving effectively decreases the error correction capacity of the (255,223) Reed-Solomon code by approximately two errors at an *SER* of $\sim 1 \times 10^{-7}$.

For the curves in Fig. 4, as well as succeeding figures below, the results are only statistically meaningful down to about 1×10^{-5} or 1×10^{-6} *SER* for the 2-Gbit datasets from Stage VIT-1. However, due to the almost parallel behavior of the depth-8 interleaving curves relative to the family of infinite interleaving curves, the depth-8 curves can be extended to 1×10^{-7} *SER* with high confidence by extrapolating along the appropriate infinite interleaving curve(s).

3. **Performance of One-Stage Decoding.** For the baseline coding system using the (255,223) Reed-Solomon code, E is 16 and a one-stage decoding system with depth-8 interleaving can achieve an *SER* of 2×10^{-7} (i.e., a *BER* of $\sim 1 \times 10^{-7}$) at convolutional code $E_b/N_o = 0.59 \text{ dB}$. This calculation assumes an extrapolation along the $E = 14$ infinite interleaving curve as discussed above. The corresponding concatenated code signal-to-noise ratio is $E_b/N_o = 1.17 \text{ dB}$, accounting for the 0.58 dB redundancy of the (255,223) Reed-Solomon code.

B. Two-Stage Decoding

For two-stage decoding with depth-8 interleaving, the performance of the Viterbi decoder in both stages is the same as that for the infinite interleaving analysis. The Reed-Solomon decoding performance is the same as that for one-stage decoding with depth-8 interleaving, to a degree of approximation noted below.

1. **Stage VIT-1.** The output of Stage VIT-1 is characterized by the performance curves given in Fig. 1.

2. **Stage RS-1.** The output of Stage RS-1 is characterized by the performance curves given in Fig. 4.

3. **Stage VIT-2.** The output of Stage VIT-2 is characterized by the same performance curves as given in Fig. 3.

4. **Stage RS-2.** The output of Stage RS-2 can be conservatively approximated by the performance curves given in Fig. 4, after using the *SER*-equivalent Stage VIT-1 operating points to characterize the output of Stage VIT-2. For the case of noninfinite interleaving, this equivalence

is not exact, because the output of Stage RS-2 depends not only on the input SEr but also on the statistics of the error bursts that contribute to the average SEr . The typical error bursts output from Stage VIT-2 were demonstrated to be much shorter than those output from Stage VIT-1 at the same value of SEr . Shorter bursts are less likely to contribute two or more symbol errors to a given interleaved codeword, and hence the performance of Stage RS-2 should be slightly better (i.e., closer to infinite interleaving performance) than that of Stage RS-1 at the same average SEr .

5. Performance of Two-Stage Decoding. If one of every four codewords is strong, extrapolation of the curves in Fig. 4 shows that a correction capability approximately halfway between $E = 32$ and $E = 34$ for the strong words is sufficient to drive $SEr_w(1)$ to about 1×10^{-7} at a convolutional code operating point of 0.20 dB. According to Figs. 3 and 4, $E = 10$ is sufficient to push $SEr_w(2)$ to 1×10^{-7} for the weak codewords at phases ± 1 and $E = 11$ can achieve $SEr_w(2) = 2 \times 10^{-7}$ for the weak codewords at phase ± 2 . The overall SEr for this scheme is approximately $1 \times 10^{-7} + (1/2)1 \times 10^{-7} + (1/4)2 \times 10^{-7} = 2 \times 10^{-7}$. The redundancy profile is (66,20,22,20) and costs 0.58 dB of overhead. The resulting concatenated code operating point is $0.20 \text{ dB} + 0.58 \text{ dB} = 0.78 \text{ dB}$.

V. Analysis Based on Depth-8 Interleaving and a Simple Erasure Declaration Rule

This section analyzes the gains possible from applying a combination of Viterbi redecoding and Reed-Solomon redecoding using erasure declarations to codewords interleaved to depth 8. The erasure declaration rule is a simple strategy modeled after one of the rules given by Belongie and Arnold¹; it is effective but not optimized. A symbol is always erased (a "double-sided" erasure) if it falls between two known erroneous symbols no more than eight symbols apart from each other. If this does not suffice to make the codeword decodable, a symbol is also erased (a "single-sided" erasure) if it is immediately adjacent to one known erroneous symbol. Single-sided erasures are extended one symbol farther (into the next adjacent codeword) every time another codeword successfully decodes. The erasure declaration process is repeated until no additional codewords are decodable within the block of eight interleaved words.

¹ M. Belongie and S. Arnold, "Error Forecasting Performance (Preliminary)," JPL Interoffice Memorandum 331-92.2-142 (internal document), Jet Propulsion Laboratory, Pasadena, California, January 4, 1993.

As with the analyses presented earlier, this section begins with a baseline analysis of one-stage decoding (no Viterbi redecoding) and proceeds to evaluate the gains possible from using a second stage. Results are not presented for more than two decoding stages.

A. One-Stage Decoding

One-stage decoding consists of one pass through the Viterbi decoder followed by one or more passes through the Reed-Solomon decoder to allow the various sequences of erasure declarations described above to be tried. The performance of the Viterbi decoder is the same as before. The performance of the Reed-Solomon decoder must be evaluated by directly measuring the ultimate probability of decoder failure after applying the rule for erasure declarations, using simulated interleaved output from the Viterbi decoder.

1. Stage VIT-1 The output of Stage VIT-1 is characterized by the performance curves given in Fig. 1.

2. Stage RS-1. Figure 5 shows the performance of the Reed-Solomon decoder under an assumption of depth-8 interleaving and the simple erasure declaration algorithm described above. For the solid curves in Fig. 5, it is assumed that all eight codewords in a frame have the same error correction capacity E , and performance is plotted for $E = 10, 16$. The $E = 16$ performance curve in Fig. 5 shows a performance gain of about 0.10 dB with respect to the corresponding curve in Fig. 4 and a gain of about 0.05 dB with respect to the curve in Fig. 2. The erasure declaration algorithm is powerful enough not only to overcome the degradation due to finite interleaving but also to outperform decoding with ideal interleaving but no erasure declarations. At low SEr , the $E = 16$ depth-8 interleaving curve with erasure declarations is almost coincident with the $E = 18$ infinite interleaving curve with no erasure declarations. Thus, depth-8 interleaving combined with Reed-Solomon redecoding using a simple erasure declaration rule effectively increases the error correction capacity of the (255,223) Reed-Solomon code at an SEr of $\sim 10^{-7}$ by approximately two errors relative to infinite interleaving with no erasure declarations, or by approximately four errors relative to depth-8 interleaving with no erasure declarations.

The dot-dash curve in Fig. 5 shows the performance of the Reed-Solomon decoder using the same erasure declaration algorithm but allowing the codewords to have the variable redundancy profile (44,28,28,28) discussed by Belongie and Arnold.² This profile has the same average

² Ibid.

redundancy as the constant redundancy code with $E = 16$ and therefore the same redundancy overhead. The SE_R curve for this variable redundancy scheme lies just under the infinite interleaving curve for $E = 20$. The effective average error correction capability is improved over the constant redundancy scheme by approximately two additional errors, or equivalently by about 0.05 dB at an SE_R of $\sim 10^{-5}$.

3. Performance of One-Stage Decoding. Extrapolation of the $E = 16$ curve in Fig. 5 yields a required operating point of 0.46 dB to achieve an $SE_R = 2 \times 10^{-7}$. This corresponds to a concatenated code operating point of 0.46 dB + 0.58 dB = 1.04 dB. The $E = 10$ curve requires 0.67 dB plus 0.35 dB of overhead or 1.02 dB for the concatenated code. The variable redundancy (44,28,28,28) code requires 0.40 dB + 0.58 dB = 0.98 dB.

B. Two-Stage Decoding

For two-stage decoding with depth-8 interleaving and Reed-Solomon erasure declarations, the performance of the Viterbi decoder in both stages is the same as before. The evaluation of Reed-Solomon decoding performance must be modified somewhat to account for the fact that erasure declarations in strong codewords in Stage RS-1 must typically be forecast only from other strong codewords (because weak codewords are not highly likely to decode during Stage RS-1), and erasures in weak codewords in Stage RS-2 must be forecast from other weak codewords (because there are no symbol errors remaining in strong codewords in Stage RS-2 from which to forecast neighboring symbol errors).

1. Stage VIT-1. The output of Stage VIT-1 is characterized by the performance curves given in Fig. 1.

2. Stage RS-1. The output of Stage RS-1 is characterized by the performance curves given in Fig. 6. These curves show the SE_R that is obtained when strong and weak codewords are intermixed within a frame, but one attempts to decode only the strong words (and declares only those erasures based on decodable strong codewords). The plotted SE_R is the average SE_R obtained by accumulating symbol errors from all the codewords in frames that contain at least one strong codeword error. The dashed curves in Fig. 6 show SE_R for a redundancy profile of one strong word every two codewords, and the thick solid curves show SE_R for one strong word every four codewords. The error correction values noted for these curves ($E_s = 26, 28$ for the first case and $E_s = 30, 32, 34$ for the second case) pertain to the strong codewords only.

3. Stage VIT-2. The output of Stage VIT-2 is characterized by the same performance curves given in Fig. 3.

4. Stage RS-2. At present no curves directly characterize the output of Stage RS-2. The SE_R from Stage RS-2 can certainly be upper bounded by the SE_R obtainable without erasure declarations, as shown in Fig. 4. The incremental effect of Reed-Solomon redecoding with erasure declarations can be estimated to some degree by comparing curves in Fig. 4 (without erasure declarations) with corresponding curves in Fig. 5 (with erasure declarations), but this is not an exact procedure because the effect of erasure declarations is different after Viterbi redecoding than after Viterbi decoding the first time. In particular, the shorter bursts from Stage VIT-2 should lead to less efficacious error forecasting than the longer bursts from the "equivalent" Stage VIT-1 operating point.

5. Performance of Two-Stage Decoding. Assume that one of every four codewords is strong, and the convolutional code operating point is 0.20 dB. Extrapolation of the curves in Fig. 6 shows that a correction capability of $E = 32$ for the strong words is sufficient to drive $SE_{R_s}(1)$ to about 1×10^{-7} . Similarly, according to Figs. 3 and 4, $E = 10$ is sufficient to push $SE_{R_w}(2)$ to the same level for the weak codewords at phases ± 1 even without any assistance from erasure declarations. For the overall SE_R to reach 2×10^{-7} , the remaining weak codewords at phase ± 2 must achieve $SE_{R_w}(2)$ of 2×10^{-7} or lower. From Figs. 3 and 4 this can be approximately accomplished without any erasure declarations by a code with $E = 11$. However, it is estimated that this required value of E can also be reduced to $E = 10$ by using erasure declarations from the codewords at phases ± 1 to help decode the words in between at phase ± 2 . The redundancy profile for this case is (64,20,20,20) and it costs 0.56 dB of overhead. The resulting concatenated code operating point is 0.20 dB + 0.56 dB = 0.76 dB.

If the convolutional code operating point is moved to 0.10 dB, the corresponding required values of E for the strong and weak codewords are approximately $E = 38$ and $E = 11$, respectively, but there are insufficient data plotted in Figs. 4 and 6 to confirm this directly. The corresponding redundancy profile is (76,22,22,22) and the concatenated code operating point is 0.75 dB, which is almost identical to the previous value. Again this indicates an insensitivity of the optimum performance to small variations on the order of 0.1 dB in the convolutional code operating point. All other things being equal, there is a slight preference to operate at the higher convolutional code E_b/N_o in order to raise the channel symbol signal-to-noise ratio.

VI. Performance Comparisons

Tables 1 and 2 summarize the optimal or near-optimal (within a few hundredths of a dB) concatenated code decoding thresholds for achieving an overall $SEER$ of 2×10^{-7} (a BER of $\sim 1 \times 10^{-7}$) for the various decoding alternatives considered in the preceding sections.

Several conclusions can be drawn from these two tables. Based on the infinite interleaving analysis, a second stage of Viterbi decoding without any Reed-Solomon redecoding is worth about 0.38 dB at $SEER = 2 \times 10^{-7}$. The same comparison for depth-8 interleaving yields essentially the same answer, 0.39 dB. Adding Reed-Solomon redecoding using erasure declarations increases this value only marginally to 0.41 dB for the case of depth-8 interleaving. This tiny incremental value of Reed-Solomon redecoding when used in conjunction with Viterbi redecoding is probably somewhat underestimated due to the conservative approximations made in the foregoing analysis, but the true incremental value is unlikely to be more than several hundredths of a dB. On the other hand, Reed-Solomon redecoding without Viterbi redecoding is worth about 0.19 dB for depth-8 interleaving.

Allowing four stages of Viterbi decoding (and four levels of Reed-Solomon redundancy) is worth about 0.58 dB for infinite interleaving and no erasure declarations. Data are not available to confirm the corresponding result for depth-8 interleaving, but a similar effect is expected.

Tables 1 and 2 also give a measure of the amount by which depth-8 interleaving is nonideal. Compared to infinite interleaving, depth-8 interleaving costs 0.06 or 0.07 dB for both one- and two-stage decoding without erasure declarations.

VII. Choosing a Coding System for Best Performance

If the objective for the Galileo LGA code is to maximize the allowable data rate, this is accomplished by lowering the concatenated code's decoding threshold as far as possible. Under a constraint of no more than two decoding stages and two levels of codeword redundancy, the best performance is obtained by using two-stage decoding with one strong codeword every four. The redundancy profile (64,20,20,20) achieves a near-optimum concatenated code decoding threshold of 0.76 dB while requiring the convolutional code to operate at 0.20 dB.

Based on the infinite interleaving analysis reported in Table 1, performance may be further improved by approximately 0.2 dB if four stages of Viterbi decoding and four levels of Reed-Solomon redundancy are permitted. Confirmation of this effect and specification of the optimum four-level redundancy profile for depth-8 interleaving will be the subject of a future article.

References

- [1] K.-M. Cheung and S. J. Dolinar, Jr., "Performance of Galileo's Concatenated Codes with Nonideal Interleaving," *The Telecommunications and Data Acquisition Progress Report 42-95*, vol. July-September 1988, Jet Propulsion Laboratory, Pasadena, California, pp. 148-152, November 15, 1988.
- [2] O. Collins and M. Hizlan, "Determinant-State Convolutional Codes," *The Telecommunications and Data Acquisition Progress Report 42-107*, vol. July-September 1991, Jet Propulsion Laboratory, Pasadena, California, pp. 36-56, November 15, 1991.

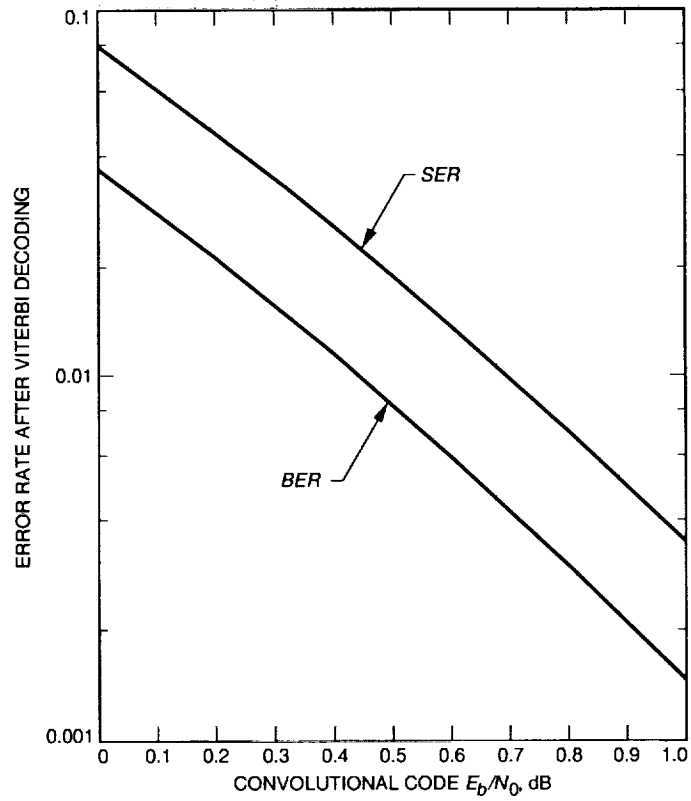


Fig. 1. Bit error rate and symbol error rate after Viterbi decoding of the (14, 1/4) Galileo LGA convolutional code.

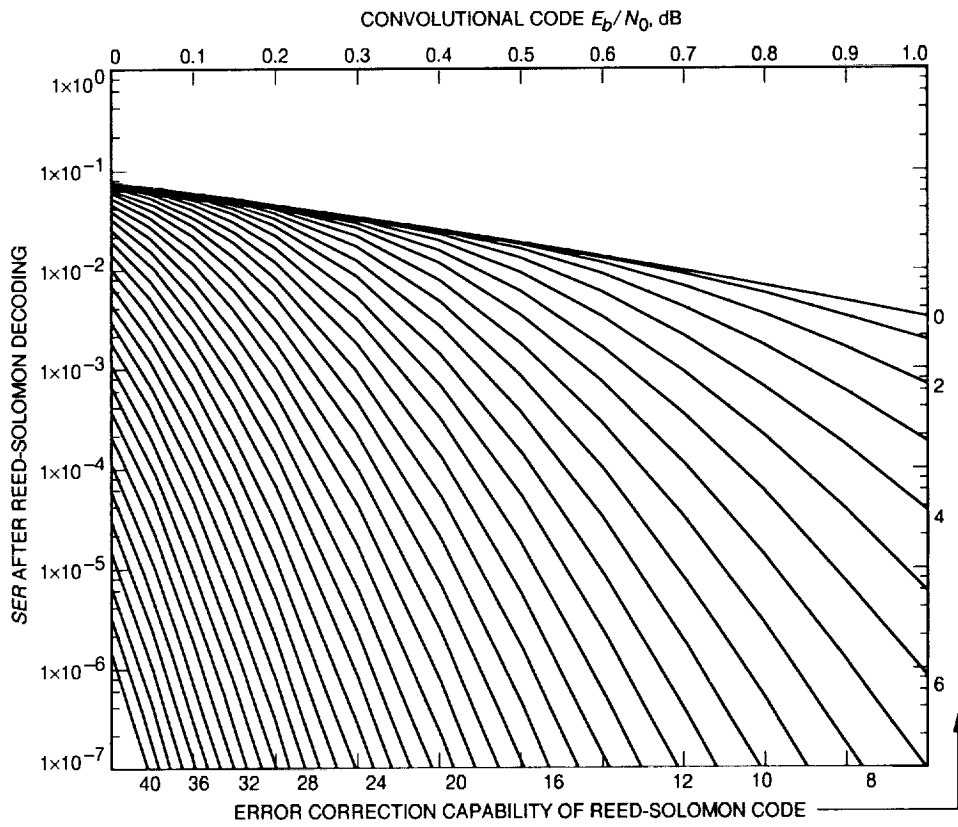


Fig. 2. Symbol error rate after Reed-Solomon decoding with infinite interleaving.

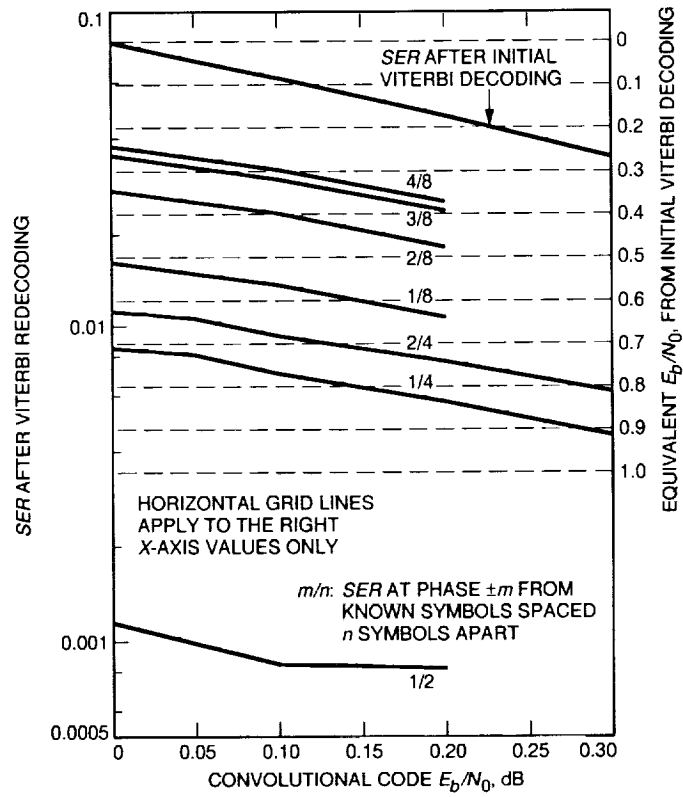


Fig. 3. Symbol error rate after Viterbi redecoding with various spacings of known symbols and relative phases of unknown symbols.

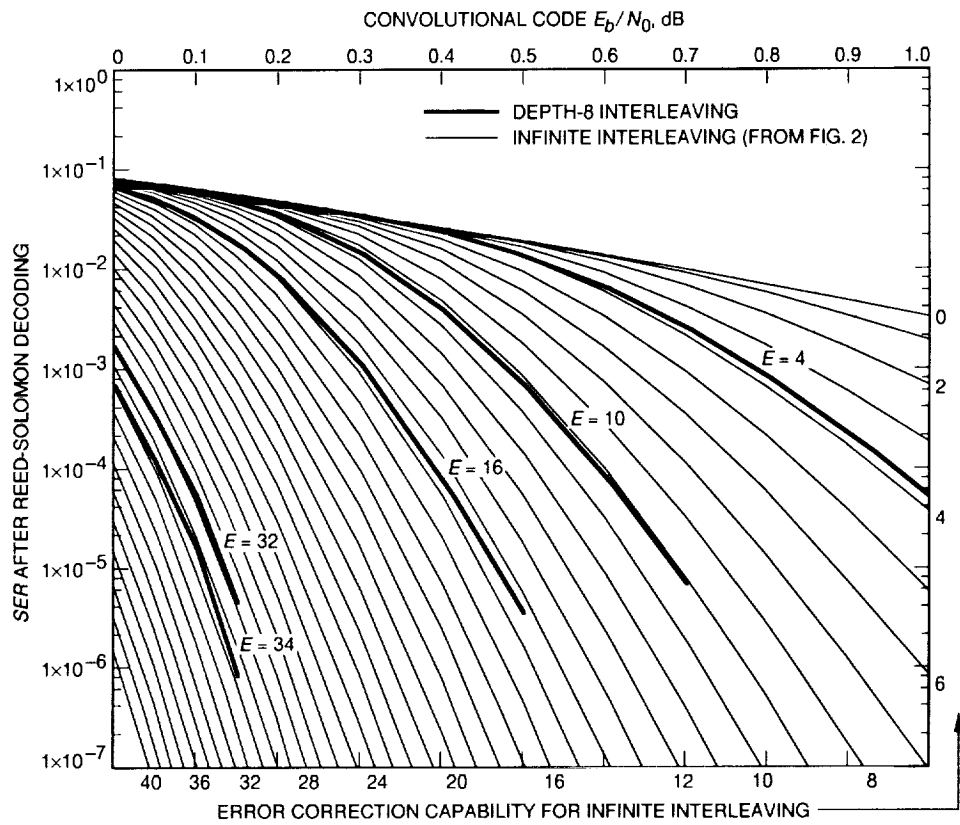


Fig. 4. Symbol error rate after Reed-Solomon decoding with depth-8 interleaving.

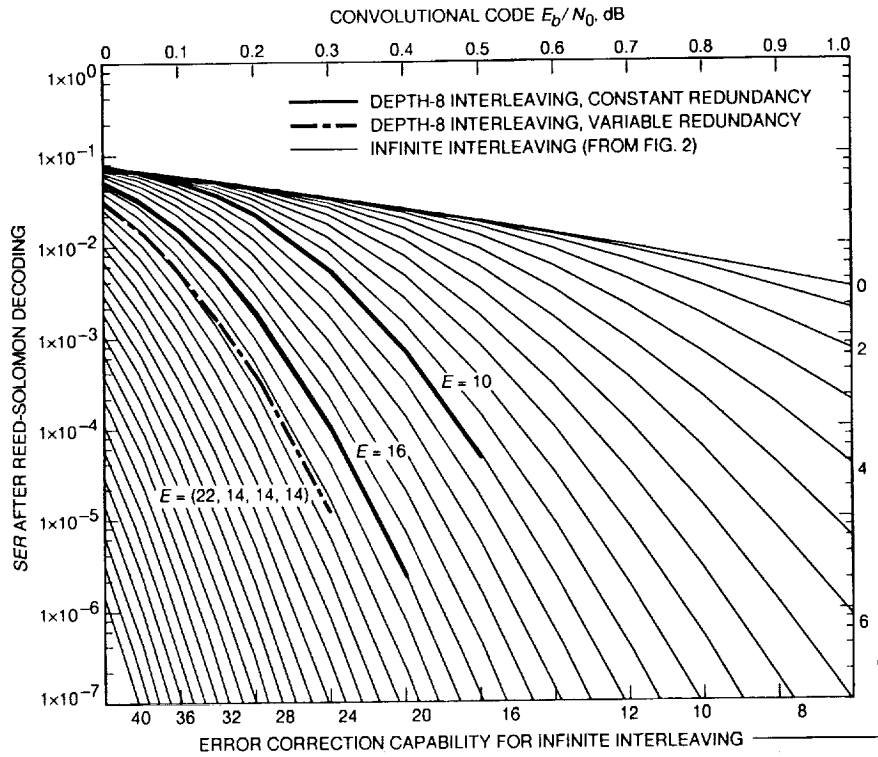


Fig. 5. Symbol error rate after Reed-Solomon decoding using erasure declarations with depth-8 interleaving.

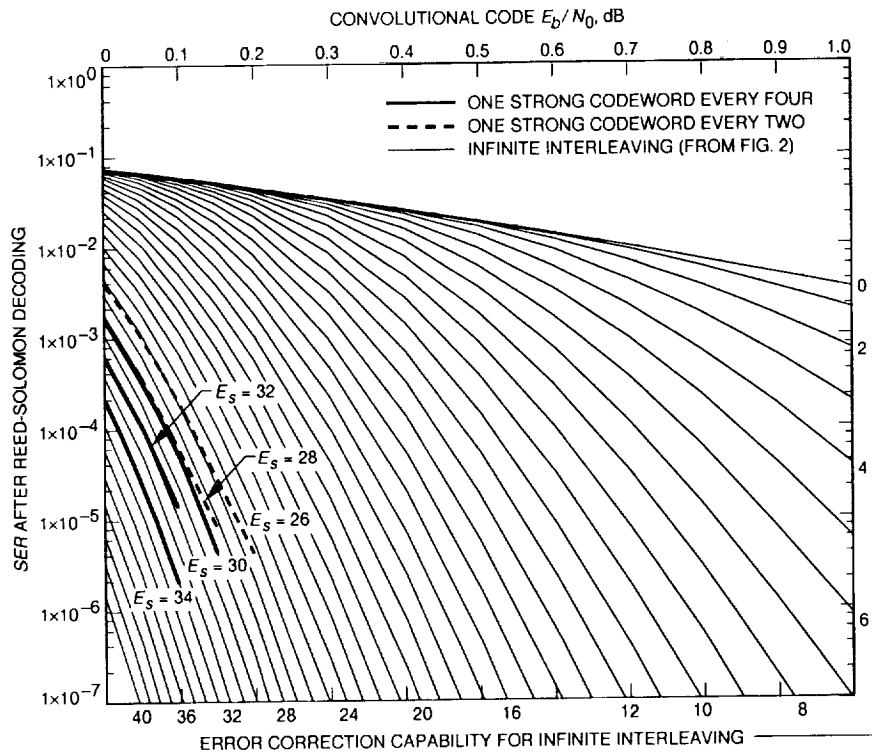


Fig. 6. Symbol error rate after Reed-Solomon decoding using erasure declarations among strong codewords only with depth-8 interleaving.

Table 1. Performance comparisons for infinite interleaving ($SE_R = 2 \times 10^{-7}$).

Decoding stages	1	2	4
Erasure declarations	No	No	No
Redundancy profile	(32)	(60, 18, 20, 18)	(86, 10, 26, 10, 54, 10, 26, 10)
Convolutional code E_b/N_0 (dB)	0.52	0.20	0.00
Concatenated code E_b/N_0 (dB)	1.10	0.72	0.52

Table 2. Performance comparisons for depth-8 interleaving ($SE_R = 2 \times 10^{-7}$).

Decoding stages	1	1	2	2
Erasure declarations	No	Yes	No	Yes
Redundancy profile	(32)	(44, 28, 28, 28)	(66, 20, 22, 20)	(64, 20, 20, 20)
Convolutional code E_b/N_0 (dB)	0.59	0.40	0.20	0.20
Concatenated code E_b/N_0 (dB)	1.17	0.98	0.78	0.76